Metrol. Meas. Syst., Vol. XXI (2014), No.3, pp. 497–508.

METROLOGY AND MEASUREMENT SYSTEMS
Index 330930, ISSN 0860-8229
www.metrology.pg.gda.pl

USING A PARTICULAR SAMPLING METHOD FOR IMPEDANCE MEASUREMENT

Grzegorz Lentka

Gdansk University of Technology, Faculty of Electronics Telecommunications and Informatics Gdansk, Poland (✉lentka@eti.pg.gda.pl)

Abstract

The paper presents an impedance measurement method using a particular sampling method which is an alternative to DFT calculation. The method uses a sine excitation signal and sampling response signals proportional to current flowing through and voltage across the measured impedance. The object impedance is calculated without using Fourier transform. The method was first evaluated in MATLAB by means of simulation. The method was then practically verified in a constructed simple impedance measurement instrument based on a PSoC (Programmable System on Chip). The obtained calculation simplification recommends the method for implementation in simple portable impedance analyzers destined for operation in the field or embedding in sensors.

Keywords: impedance measurement, impedance analyzer, particular sampling.

1. Introduction

There are many technical and biological objects, the parameters of which can be determined by impedance measurement. An example of such approach is monitoring and diagnostics of anticorrosion protection of large technical objects like pipelines, bridges, fuel tanks etc. on the basis of impedance measurement of the protective anticorrosion coatings [3, 4]. An example of environmental protection and safety is the use of impedance measurement for monitoring of water percolation of dikes [5–7]. Another example is sensing technology e.g. relative humidity sensors [8]. In case of the first two examples there is a need of distributed measurements in many places – numerous sensors are required, so the measurement time is extended meaningfully or the required number of instruments working in parallel becomes higher. In case of sensors, the total cost of the device, circuit dimensions and power consumption should be kept as small as possible mainly due to economic reasons. The above presented guidelines lead to searching for new methods which allow to simplify impedance measurement instruments, allowing further simplification and miniaturization than solutions presented in [9–11]. The previous works in the author's team were addressing this problem by reducing the number of samples taken into calculations [12].

2. Impedance measurement method

In order to measure impedance, the single sine technique (SST) is commonly used. By repeating the measurements at different frequencies, the impedance spectrum can be obtained directly from measurement results as a function of frequency in a range of a few decades. SST is based on excitation of the object with a harmonic signal and vector measurement of two signals: voltage across and current through the measured object (Fig. 1).

Article history: received on Feb. 15, 2014; accepted on Mar. 28, 2014; available online on Sep. 15, 2014; DOI: 10.2478/mms-2014-0042.

In the digital implementation of the impedance measurement method [13], excitation signal u_g is produced with the aid of Direct Digital Synthesis (DDS) using a D/A converter and memory containing sine samples. To extract signals proportional to the voltage across (u_u~u_x) and current through (u_i~i_x) the measured impedance Z_x the input circuitry has to be used. The construction of the input circuit is very important as parasitic capacitances and real-life parameters of the operational amplifiers can significantly influence a measurement result [14]. Signals u_u and u_i are sampled synchronously with the clock generator using two A/D converters and placed in memory in the form of two sets of N samples of signals $u_u[n]$ and $u_i[n]$.

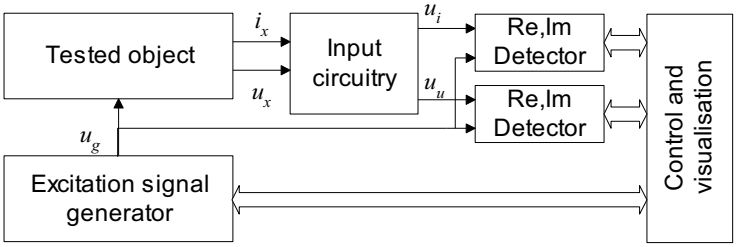

Fig. 1. Block diagram of the impedance measurement system.

To determine the orthogonal parts of the acquired signals on the basis of the collected samples, different techniques can be used: the use of Fourier transformation (DFT or FFT) [13], sine-fitting algorithms [15], ellipse fitting algorithms [16] and others. When classifying the above mentioned algorithms according to the memory usage, the DFT/FFT algorithms present the smallest memory usage – calculations can be performed "in-place", using the same memory space which is used by signal samples. Sine-fitting algorithms need extra additional memory space for matrix calculations or even require many iterations in case of 4- and 7-parameter fitting algorithms. Usually, for implementing sine-fitting algorithms, at least a 32-bit processing unit is required [15], but for some applications such strong CPU is not necessary, an 8-bit architecture should be enough and more efficient from the energetic viewpoint.

Using classical DFT [17], on the basis of the collected samples and assuring the conditions: the sampled signal is sinusoidal and the collected samples contain an integer number L of the measurement signal periods, the orthogonal parts of the L-line of the measurement signals U_u and U_i spectrum can be determined according to formulas:

$$\begin{aligned} \mathrm{Re}(U_u^L) &= \sum_{m=0}^{N-1} u_u^m \cdot \cos\left(\frac{2\pi \cdot m \cdot L}{N}\right), \quad \mathrm{Im}(U_u^L) = \sum_{m=0}^{N-1} u_u^m \cdot \sin\left(\frac{2\pi \cdot m \cdot L}{N}\right) \\ \mathrm{Re}(U_i^L) &= \sum_{m=0}^{N-1} u_i^m \cdot \cos\left(\frac{2\pi \cdot m \cdot L}{N}\right), \quad \mathrm{Im}(U_i^L) = \sum_{m=0}^{N-1} u_i^m \cdot \sin\left(\frac{2\pi \cdot m \cdot L}{N}\right) \end{aligned} . \tag{1}$$

Using orthogonal parts of signals proportional to voltage across and current through the measured object calculated according to (1), on the basis of impedance definition, the impedance modulus and argument are calculated according to:

$$|Z_x| = \sqrt{\frac{(\mathrm{Re}\,U_u)^2 + (\mathrm{Im}\,U_u)^2}{(\mathrm{Re}\,U_i)^2 + (\mathrm{Im}\,U_i)^2}}\, R_R, \quad \varphi_{Z_x} = \mathrm{arctg}\frac{\mathrm{Im}\,U_u}{\mathrm{Re}\,U_u} - \mathrm{arctg}\frac{\mathrm{Im}\,U_i}{\mathrm{Re}\,U_i}, \tag{2}$$

where: R_R – range resistor in the input circuitry, scaling current-to-voltage conversion.

Although the impedance measurement using DFT algorithms does not use an additional space (above that required for sample storage), some drawbacks of the method exist. The number of samples used for calculations is relatively high. In the hardware realization of DFT for impedance measurement (AD5933 [18]), the samples number is equal to 1024, for software realization, the required memory size (1024samples*2channels*2bytes/sample = 4096) is relatively high. Additionally, the number of calculations (multiplications and additions) is also directly connected with the sample number. This leads to relatively high required processing power and high memory use, which cannot be available on the small, low power microcontrollers designed be used in applications mentioned in the Introduction.

As a remedy, the particular sampling method invented by Prof. Sawicki [1, 2] is used for determining the orthogonal parts of the measurement signals.

3. Particular sampling method implementation

The particular sampling method is based on taking signal samples in precisely determined time moments, allowing to simply calculate the vector of fundamental harmonic of the measurement signal. When comparing to DFT, the particular sampling method uses only a summation of the collected samples, and the obtained two sums determine the orthogonal parts of the measured sinusoidal signal. A precise theoretical description and discussion of the method is presented in [1, 2] and here only the most important aspects will be recalled.

If we assume that the measurement signal is a distorted sinusoidal signal, the k-th harmonic can be described by a Fourier series with coefficients:

$$u(x) = U_0 + \sum_{k=1} U_k \sin(\alpha_k + k \cdot x), \tag{3}$$

where: U_0 – DC component, U_k, α_k, T – k-th harmonic amplitude, phase shift, period, $x = \frac{2\pi \cdot t}{T}$.

In order to eliminate U_0, we acquire samples at two time moments: x and $(x + \frac{180}{n})$ and subtract each other, as shown in the formula:

$$u(x) - u(x + \frac{180}{n}) = \sum_{j=1}^{2} (-1)^{1+m} u(x + \frac{m \cdot 180}{n}), \text{ where: } m = (j-1) \oplus 2, \oplus \text{ - modulo operation.} \tag{4}$$

Using addition theorems of trigonometric functions shown in:

$$\sin\alpha - \sin\beta = 2\sin(\frac{\alpha - \beta}{2})\cos(\frac{\alpha + \beta}{2}), \quad \cos\alpha + \cos\beta = 2\cos(\frac{\alpha - \beta}{2})\cos(\frac{\alpha + \beta}{2}), \tag{5}$$

formula (4) can be written as:

$$\sum_{j=1}^{2} (-1)^{1+m} u(x + \frac{m \cdot 180}{n}) = 2\sum_{k=1} U_k \sin\frac{k \cdot 90}{n} \cos\left[\alpha_k + k \cdot (x + \frac{90}{n})\right], \tag{6}$$

Writing an analogous difference for time $(x+\frac{180}{q_1})$ and $\left[(x+\frac{180}{q_1})+\frac{180}{n}\right]$, gives the formula:

$$\sum_{j=1}^{2}(-1)^{1+m}u(x+\frac{m\cdot 180}{n}+\frac{180}{q_1})=2\sum_{k=1}U_k\sin\frac{k\cdot 90}{n}\cos\left[\alpha_k+k\cdot(x+\frac{90}{n}+\frac{90}{q_1})\right]. \quad (7)$$

Summing (6) and (7) and applying (5), one can write down the formula:

$$\sum_{j=1}^{4}(-1)^{1+m}u(x+\frac{m\cdot 180}{n}+\frac{p_1\cdot 180}{q_1})=4\sum_{k=1}U_k\sin\frac{k\cdot 90}{n}\cos\frac{k\cdot 90}{q_1}\cos\left[\alpha_k+k\cdot(x+\frac{90}{n}+\frac{90}{q_1})\right], \quad (8)$$

where: $p_1=\left\lfloor(\frac{j-1}{2})\right\rfloor\oplus 2$.

Performing more iterations given by (8), high order sums can be written as in:

$$\sum_{j=1}^{2^{1+Q}}(-1)^{1+m}u(x+\frac{m\cdot 180}{n}+\frac{p_1\cdot 180}{q_1}+\frac{p_2\cdot 180}{q_2}+\ldots+\frac{p_Q\cdot 180}{q_Q})=\sum_{k=1}C_Q(k)U_k\cos\left[\alpha_k+k\cdot(x+\beta_Q)\right], \quad (9)$$

where: Q – number of used q_i factors, $p_i=\left\lfloor(\frac{j-1}{2^i})\right\rfloor\oplus 2$, $C_Q(k)=2^{1+Q}(\sin\frac{k\cdot 90}{n})\prod_{i=1}^{Q}(\cos\frac{k\cdot 90}{q_i})$ and $\beta_Q=\frac{90}{n}+\sum_{i=1}^{Q}\frac{90}{q_i}$.

When analyzing formula (9), it can be noted that the unwanted harmonics can be eliminated by proper setting m, n, p and q factor values, e.g. for $n=1$ all even harmonics will be eliminated ($C_\mathrm{Q}=0$). Odd harmonics can be eliminated by proper selection of q_i values. Each q_i, which removes the k-th harmonic, also removes its odd multiple. Table 1 presents example values of q_i, as it can be noted [1], the higher the Q value, the better the harmonics elimination. On the other hand, the higher the Q value, the higher the number of samples to be acquired. Practically, for $Q=2$, we obtain quite good harmonics elimination.

Table. 1. Example q_i values and eliminated harmonics.

q_i	Eliminated harmonics
3	3, 9, 15, 21, 27, 33, 39, 45, 51,…
5	5, 15, 25, 35, 45, 55, 65, 75,…
7	7, 21, 35, 49, 63, 77,…
11	11, 33, 55, 77, 99,…
13	13, 39, 65, 91,…
17	17, 51, 85,…
19	19, 57, 95,…
23	23, 69,…

Assuming that the measurement signal contains only those harmonics we can eliminate, the right side of formula (9) can be rewritten as:

$$C_Q(1)U_1\cos(\alpha_1 + x + \beta_Q), \tag{10}$$

Orthogonal parts of the measurement signal (Re, Im) can be determined according to formulas:

$$\mathrm{Re} = C_Q(1)U_1\cos(\alpha_1 + x + \beta_Q) = \sum_{j=1}^{2^{1+Q}} (-1)^{1+m} u(x + m180 + \frac{p_1 180}{3} + \frac{p_2 180}{5} + \ldots), \tag{11}$$

$$\mathrm{Im} = -C_Q(1)U_1\sin(\alpha_1 + x + \beta_Q) = \sum_{j=1}^{2^{1+Q}} (-1)^{1+m} u(x + 90 + m\cdot 180 + \frac{p_1 \cdot 180}{3} + \frac{p_2 \cdot 180}{5} + \ldots). \tag{12}$$

To determine orthogonal parts of voltage u_u and current u_i proportional signals we need to acquire samples and calculate two sums for each signal. Each sum components have "+" or "-" signs depending on parameter m. For easier implementation, we separate components of each sum for those with "+" sign ($\mathrm{Re_P}$ and $\mathrm{Im_P}$) and those with "-" sign ($\mathrm{Re_M}$ and $\mathrm{Im_M}$).

Formulas (11) and (12) serve as a basis to create a sampling schedule. Because the main aim for this implementation of the particular sampling algorithm is determination of the orthogonal parts of the fundamental harmonic, but not removing the possibly high number of higher harmonics, so the Q was assumed as equal 2 and according to Table 1: $q_1 = 3$ and $q_2 = 5$.

To correctly realize the particular sampling method (to sample at correct time moments) it is necessary to assure the sampling frequency f_s is related to measurement frequency f:

$$V = \frac{f_s}{f} = 4\prod_{i=1}^{Q} q_i, \tag{13}$$

For assumed values of Q=2, q_1=3 and q_2=5 the formula can be evaluated as below:

$$V = \frac{f_s}{f} = 4\prod_{i=1}^{2} q_i = 4 \cdot 3 \cdot 5 = 60, \tag{14}$$

and this means that for the assumed parameters, the sampling frequency should be 60 times higher than the measurement frequency – we need to acquire 60 samples during a measurement signal period. Using the defined V value, we can express sampling moments as a sample number by entering an variable D (given in degrees).

$$D = \frac{360}{V}[\text{deg}], \tag{15}$$

Using the formulas (11) and (12) and defined variable D, the sampling schedule can be defined as written in Table 2.

Table. 2. Sampling schedule for the proposed particular sampling method implementation.

Sum iteration number	Sampling moment according to (11) and (12)		Sampling moments expressed as D multiple – sample number			
	Re component	Im component	Re_P	Re_M	Im_P	Im_M
1	$-x$	$-(x+90)$		1		15
2	$x+180$	$x+90+180$	30		45	
3	$-(x+\frac{180}{3})$	$-(x+90+\frac{180}{3})$		10		25
4	$x+180+\frac{180}{3}$	$x+90+180+\frac{180}{3}$	40		55	
5	$-(x+\frac{180}{5})$	$-(x+\frac{180}{5})$		6		21
6	$x+180+\frac{183}{5}$	$x+90+180+\frac{183}{5}$	36		51	
7	$-(x+\frac{180}{3}+\frac{180}{5})$	$-(x+90+\frac{180}{3}+\frac{180}{5})$		16		31
8	$x+180+\frac{180}{3}+\frac{180}{5}$	$x+90+180+\frac{180}{3}+\frac{180}{5}$	46		61==1	

The sample numbers given in Table 2 can be directly used in microcontroller software for calculation of Re and Im parts of both measurement signal u_u and u_i.

4. Particular sampling method implementation test by simulation

The particular sampling method presented in Section 3 was first implemented as a Matlab script and tested. As a reference the DFT-based method was used assuming the same sampling frequency: all acquired samples containing one period of the measurement signal were used for DFT, but selected (see Table 2) samples were used for the particular sampling

method. To create a simulation situation similar to the real-life one, the generated sinusoidal signal has a white-noise signal (normal distribution) and 50 Hz noise added (reflecting interference caused by power lines).

In the first step, the influence of the white-noise amplitude (expressed as standard deviation) with zero mean value was tested. The measurement signals have a constant amplitude of 200 mV. As the particular sampling method is suspected to be more dependent on noise, the simulation was performed in series (100 realization each). For each realization, the relative impedance modulus error and absolute impedance argument errors were calculated, then for all realizations the standard deviations for modulus and for argument were calculated. Exemplary voltage and current signals for highest noise contents are presented in Fig.2 and results of the simulation are presented in Fig. 3.

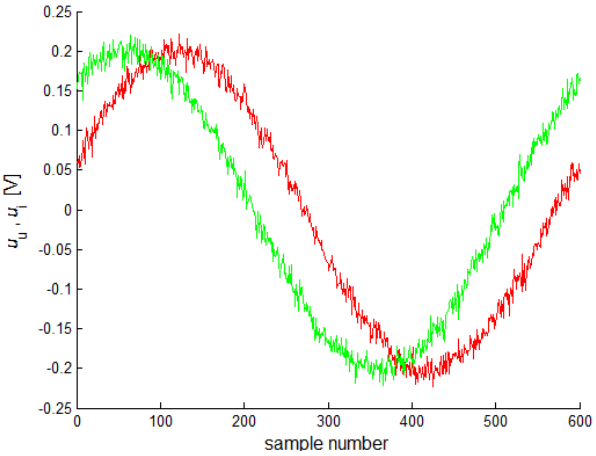

Fig. 2. Current (green) and voltage (red) signals with the highest noise contents used in the simulation.

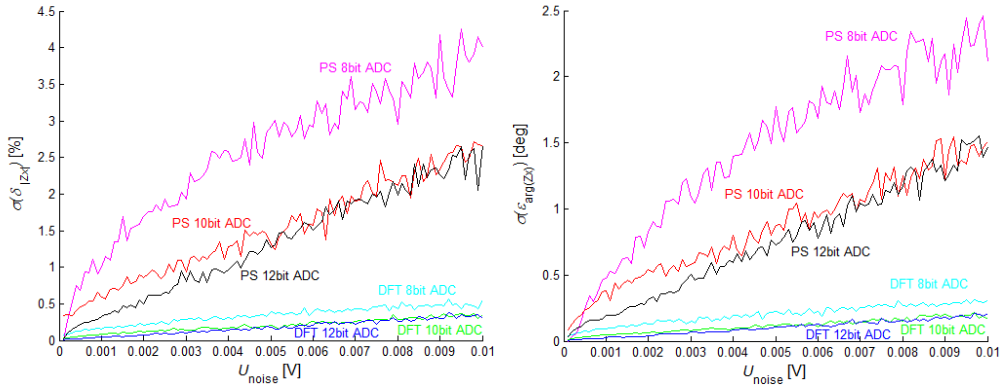

a) b)

Fig. 3. Standard deviation of relative modulus error (a) and standard deviation of absolute argument error (b) as a function of noise amplitude for particular sampling (PS) and DFT (DFT) based methods for different ADC resolutions (8, 10, 12 bits).

When analysing the graphs it can be noted that for the particular sampling method, the influence of the introduced white noise is a few times greater. The smaller the ADC resolution the worse the situation, but increasing the resolution above 12-bit does not improve the situation.

In the second step, the influence of the 50 Hz interference was evaluated, the white-noise signal standard deviation was set to 1 mV and ADC resolution to 16 bit. The frequency of "the 50 Hz" interference was changed from 49.5 up to 50.5 Hz. The errors are shown in Fig. 4.

When analyzing graphs, it can be noted that for the particular sampling method errors differs with a noise frequency change and are several times greater. It is due to the method's idea, it eliminates only harmonics taken into account. The user must be aware of this unwanted effect.

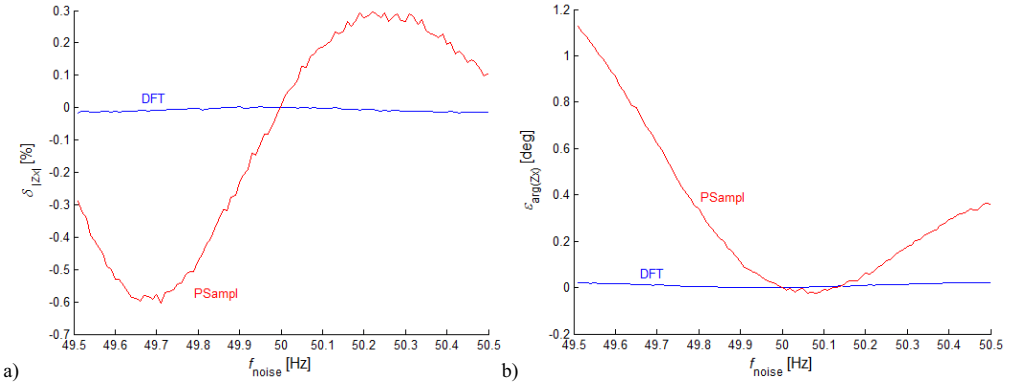

Fig. 4. Relative modulus error (a) and absolute argument error (b) as a function of '50 Hz interference' frequency for particular sampling (PSampl)- and DFT (DFT)-based methods.

For the arbitrary selected frequency of interference (50.1 Hz), the influence of its amplitude was evaluated (Fig. 5). As the 50 Hz interference amplitude increases, for the particular sampling method errors increase and are several times greater than in the DFT method.

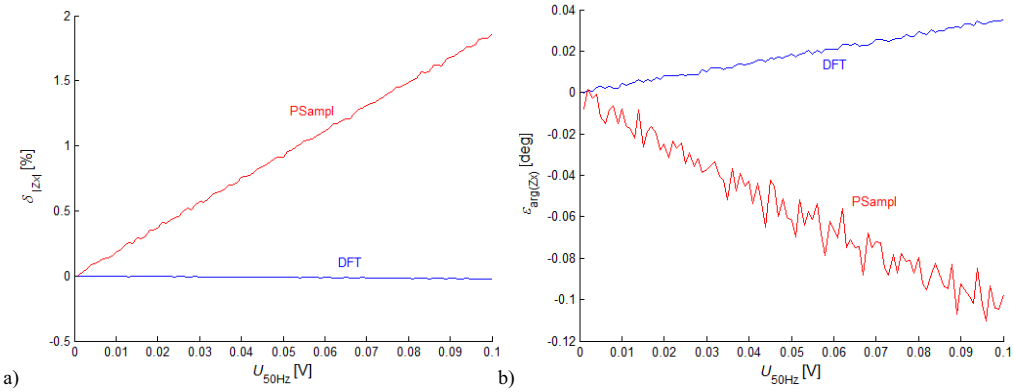

Fig. 5. Relative modulus error (a) and absolute argument error (b) as a function of 50 Hz interference amplitude for particular sampling (PSampl)- and DFT (DFT)-based methods.

5. Particular sampling-based impedance measurement method implementation in PSoC

A block diagram and a view of the measurement system prototype for experimental evaluation of the particular sampling method implementation are shown in Fig. 6. The system consists of 3 parts: a PC computer which allows to control the device and visualize/store results, the input circuitry [14], and a vector measurement unit realized using Cypress PSoC.

Thanks to the use of PSoC, the number of components was reduced to the minimum. The used PSoC generation [19] represents microcontrollers with relatively low processing power and small RAM memory. The prototype was built using a CY8C29566 chip with 2 kB SRAM memory.

The sinusoidal excitation signal u_g applied to the measured impedance is produced using the DDS method with the aid of a D/A converter DAC1, on the basis of sine samples placed in PSoC's RAM memory (GENbuf). TIMER1 creates a clock signal which controls generation and acquisition using the microcontroller clock. The DAC1 output signal before application to the impedance under test is first filtered in a low-pass filter removing unwanted stair-steps.

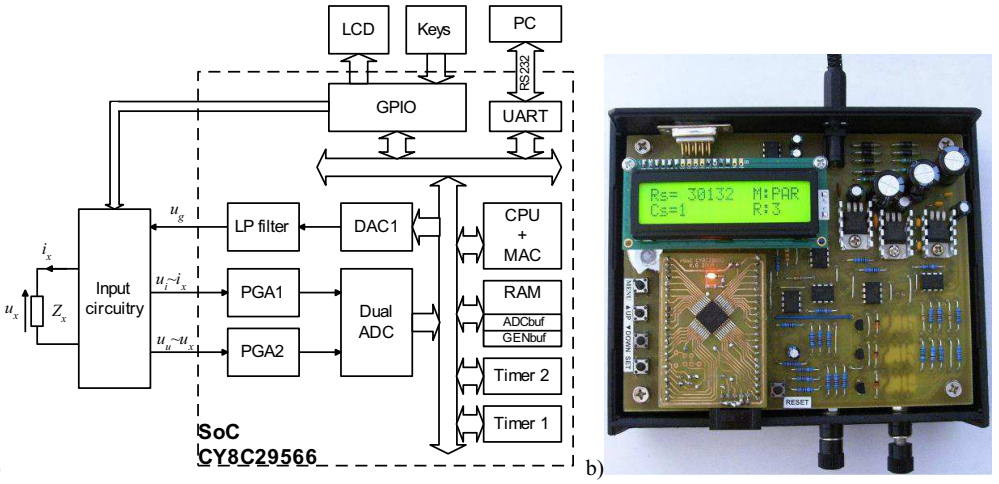

Fig. 6. Block diagram (a) and a view of prototype (b) of the particular sampling method PSoC implementation.

In the input circuitry, two signals u_i and u_u proportional to current through and voltage across the measured impedance are extracted. The extracted signals can be additionally amplified and filtered in PGA1/PGA2 blocks realized using internal PSoC blocks (amplifiers and filters). The preconditioned current and voltage signals are applied to the dual 10-bit analog-to-digital converter DUAL ADC, which synchronously samples both signals. The signal samples are stored in ADCbuf placed in a RAM memory of the PSoC microcontroller. When the sampling cycle is finished (after acquisition of the required sample number), microcontroller CPU calculates orthogonal parts Re/Im for both measurement signals on the basis of some selected samples (in case of the particular sampling method) or on the basis of collected samples and samples of sine/cosine stored in GENbuf (in case of the DFT based method). When necessary, calculations can be supported by MAC (Multiply and Accumulate) unit of the PSoC microcontroller.

6. Experimental results

In order to verify simulation results, the measurements have been performed using a realized laboratory measurement system (Fig. 6) and reference RC components whose values were measured using a Precision LCR Meter E4980A (Table 3).

Table. 3. The reference RC components used for testing the method in the system prototype.

R [Ω]		C [F]	
Nominal	**Measured**	**Nominal**	**Measured**
33	33.031	100 p	99 p
1 k	991.5	1 n	1.06 n
10 k	9.94 k	9.1 n	9.16 n
100 k	99.04 k	510 n	503.6 n
1.5 M	1.474 M	10 u	10.58 u

For each component, 100 measurement series have been performed, then the mean value and standard deviation were calculated and are presented in Fig. 7 (for resistors) and in Fig. 8 (for capacitors). The measurements were performed for different frequencies in the range of 10 Hz -1 kHz (graphs show results for 200 Hz, others were similar). The frequency range is limited due to the maximum sampling frequency of the PSoC A/D converter.

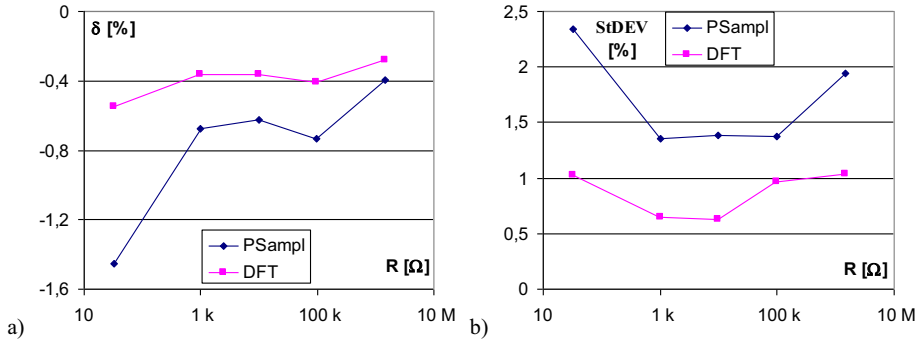

Fig. 7. Relative error (a) and relative standard deviation (b) of measurement of the reference resistors.

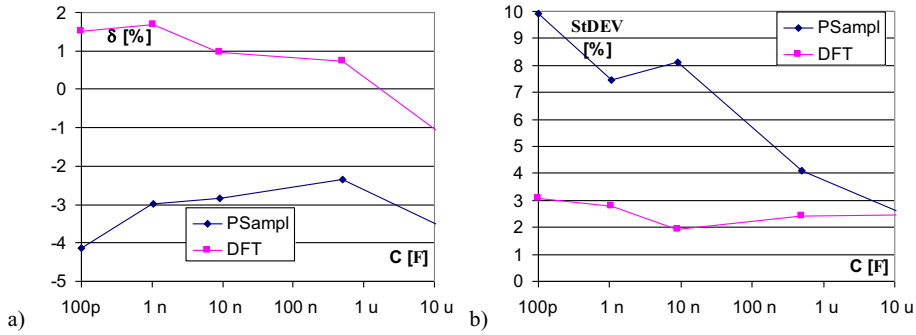

Fig. 8. Relative error (a) and relative standard deviation (b) of measurement of the reference capacitors.

The obtained results, shown in Fig. 7 and 8, are similar to simulation results. For the DFT method measurement errors are in a range of 0.5% (for resistors) and 2% (for capacitors) and for the particular sampling 1.5% and 4.2%, respectively. It should be also noted that for the particular sampling, a much greater standard deviation was observed – it is due to the nature of the method. It is worth to underline that only 60 samples (for the DFT method) and only 16

samples (for the particular sampling) were used. For capacitors, the errors are a few times greater, it results from weak filtering of the generated sine-wave – in the excitation signal still steps exist which are differentiated in the differentiating circuit created from the tested capacitor and the current-to-voltage converter in the input circuitry [14]. The obtained measurement accuracy of the developed method is acceptable in some field measurements.

7. Conclusions

The use of the particular sampling method for impedance measurement allows to meaningfully decrease the number of samples and the calculation effort. For example, for the proposed realization only 8 samples for each part (Re, Im) of each signal (voltage, current) are acquired and than added. On the other side, the accuracy of the method as well as the immunity to noise is lower than in the DFT-based impedance measurement. The obtained accuracy is acceptable in case of measurement in the field and the resulting simplification of the device can open a new application area for impedance measurement (e.g. smart impedance sensors).

The developed system is a prototype, which has made possible experimental verification of the method using particular sampling. The system has created a base for development of a simple, small impedance meter for field conditions and will be the aim of further works.

References

[1] Sawicki, J. (1988) The Finding of the Vector of the Fundamental Harmonic by the Method of a Particular Sampling, *Proc. Of 11th IMEKO Triennial World Congress "Instrumentation for the 21st Century"*, Houston, USA, Vol. Applications, 581–589.

[2] Sawicki, J. (1989) The Finding of the Vector of the Third Harmonic Component by the Method of a Particular Sampling, *Proc. 3RD IMEKO TC-4 Int. Symp. on Measurement in Electrical and Electronic Power Systems*, Zurich Switzerland, Sept. 20–22, 1–9.

[3] Skale, S., Doležek, V., Slemnik, M. (2008). Electrochemical impedance studies of corrosion protected surfaces covered by epoxy polyamide coating systems, *Prog. Organic Coat.*, (62), No. 12, 2456–2460.

[4] Bordzilowski, J., Darowicki, K., Krakowiak, S., Krolikowska, A., (2003). Impedance measurements of coating properties on bridge structures, *Progress in Organic Coatings*, Vol. 46, 216–219.

[5] Krejci, I., Parilkowa, J. (2005) Electrode Systems and Their Switching Used in Monitoring of Dike Status, *Proc. 10-th IMEKO TC10 Int. Conf. on Technical Diagnostics*, Budapest, Hungary, 2005, 63–65.

[6] Krejci, I., Parilkowa, J. (2005) Impedance Spectrometer for in situ Dike Monitoring, *Proc. of 14-th IMEKO TC-4 Int. Symp. on New Technologies in Meas. and Instrumentation*, Jurata, 2005, 283–288.

[7] Parilkowa, J., Krejci, I, Vesely, J. (2005) Two Non-invasive Methods of Dike Monitoring and Their Results, *Proc. 10-th IMEKO TC10 Int. Conf. on Technical Diagnostics*, Budapest, Hungary, 2005, 67–71.

[8] Chachulski, B., Gębicki, J., Jasiński, G., Jasiński, P., Nowakowski, A. (2006) Properties of a polyethyleneimine-based sensor for measuring medium and high relative humidity, *Meas. Sci. Technol.*, Vol. 17, No. 1, 12–16.

[9] Angelini, E., Carullo, A., Corbellini, S., Ferraris, F., Gallone, V., Grassini, S., Parvis, M., Vallan, A. (2006). Handheld-impedance-measurement system with seven-decade capability and potentiostatic function. *IEEE Trans. Instrum. Meas.*, vol. 55, no. 2, Apr. 2006, 436–441.

[10] Santos, J., Ramos, P. (2011) DSPIC-Based Impedance Measuring Instrument. *Metrology and Measurement Systems*. Vol. XVIII, Issue 2, pp. 185–198.

[11] Hoja, J., Lentka G. (2010). Interface circuit for impedance sensors using two specialized single-chip Microsystems. *Sensors and Actuators A-physical*, Vol. 163, No. 1, 191–197.

[12] Hoja, J., Lentka G. (2011). Method using square-pulse excitation for high-impedance spectroscopy of anticorrosion coatings, *IEEE Transactions on Instrumentation and Measurement*, Vol. 60, 957–64.

[13] Hoja, J., Lentka, G., Zielonko, R. (2002) Measurement microsystem for high impedance spectroscopy of anticorrosion coatings, *Metrology and Measurement Systems*, Vol. 9, No 1, 31–44.

[14] Hoja, J., Lentka, G. (2007) New concept of the measurement probe for high impedance spectroscopy, *Metrology and Measurement Systems*, Vol. 14, No. 4, 543–554.

[15] Ramos, P. M., Radil, T., Janeiro, F. M. (2012) Implementation of sine-fitting algorithms in systems with 32-bit floating point representation, *Measurement*, Vol. 45, No. 2, 155–163.

[16] Ramos, P., Janeiro, F., Radil, T. (2010) Comparative Analysis of Three Algorithms for Two-Channel Common Frequency Sinewave Parameter Estimation: Ellipse Fit, Seven Parameter Sine Fit and Spectral Sinc Fit. *Metrology and Measurement Systems*. Vol. 17, Issue 2, pp. 255–270.

[17] Smith, W. H. (1999) The Scientist and Engineer's Guide to Digital Signal Processing, *California Technical Publishing*, San Diego, USA, 1999.

[18] Analog Devices (2005) Datasheet: AD5933 1 MSPS, 12-Bit Impedance Converter, Network Analyzer.

[19] Cypress Semiconductor (2013) PSoC™ Mixed Signal Array Technical Reference Manual, Rev. H.